Available online at www.sciencedirect.com
ScienceDirect
Biochimica et Biophysica Acta 1767 (2007) 381–386
Biochimica et Biophysica Acta BBA
www.elsevier.com/locate/bbabio

The inside pH determines rates of electron and proton transfer in vesicle-reconstituted cytochrome *c* oxidase

Kristina Faxén, Peter Brzezinski *

Department of Biochemistry and Biophysics, The Arrhenius Laboratories for Natural Sciences, Stockholm University, SE-106 91 Stockholm, Sweden

Received 10 January 2007; received in revised form 26 February 2007; accepted 27 February 2007
Available online 14 March 2007

Abstract

Cytochrome *c* oxidase is the terminal enzyme in the respiratory chains of mitochondria and many bacteria where it translocates protons across a membrane thereby maintaining an electrochemical proton gradient. Results from earlier studies on detergent-solubilized cytochrome *c* oxidase have shown that individual reaction steps associated with proton pumping display pH-dependent kinetics. Here, we investigated the effect of pH on the kinetics of these reaction steps with membrane-reconstituted cytochrome *c* oxidase such that the pH was adjusted to different values on the inside and outside of the membrane. The results show that the pH on the inside of the membrane fully determines the kinetics of internal electron transfers that are linked to proton pumping. Thus, even though proton release is rate limiting for these reaction steps (Salomonsson et al., *Proc. Natl. Acad. Sci.* USA, 2005, 102, 17624), the transition kinetics is insensitive to the outside pH (in the range 6–9.5).

Keywords: *Rhodobacter sphaeroides*; Proton pumping; Cytochrome aa_3; Respiration; Kinetics

1. Introduction

Cytochrome *c* oxidase (Cyt*c*O) is the last component of the respiratory chain in the inner mitochondrial membrane in eukaryotes and the cytoplasmic membrane of prokaryotes where it catalyzes the reduction of dioxygen to water:

$$4e^- + 4H^+ + O_2 - - - > 2\ H_2O \quad (1)$$

The protons and electrons used to form water are taken up from the more negative (*N*-) and the more positive (*P*-) side of the membrane, respectively, which results in a charge separation that contributes to maintaining a proton electrochemical gradient across the membrane. In addition, the reaction drives proton translocation across the membrane from the *N*- to the *P*- side, further contributing to the electrochemical gradient that is used, for example, to produce ATP (for recent reviews, see [1–4]).

The *Rhodobacter sphaeroides* Cyt*c*O (cytochrome aa_3) contains four redox-sites (Fig. 1): Cu_A, heme *a* and the catalytic site composed of heme a_3 and Cu_B [5,6]. The two heme groups, as well as Cu_A display redox-dependent absorbance changes in the visible-near infrared region, which enables studies of electron transfer through the Cyt*c*O using time-resolved optical absorption spectroscopy. During Cyt*c*O turnover, electrons are initially delivered by cytochrome *c* to Cu_A, and then consecutively to heme *a* and the catalytic site, consisting of heme a_3 and Cu_B.

In the present investigation we have studied the reaction of the fully reduced (by four electrons) Cyt*c*O with O_2. In this experiment the reduced Cyt*c*O is incubated under an atmosphere of CO, which binds to heme a_3 at the catalytic site preventing binding of oxygen. Flash photolysis of the ligand in the presence of oxygen allows initiation of the reaction with O_2 simultaneously in the entire enzyme population. After O_2 binding to Cyt*c*O from *R. sphaeroides* [7] an electron is transferred from heme *a* to heme a_3 with a time constant of ~50 μs. On the same time scale the O–O bond is broken and an intermediate called $\mathbf{P^3}$ is formed (the superscript denotes the number of electrons delivered to the catalytic site). In the next reaction step a proton is transferred from the *N*-side solution to the catalytic site, forming intermediate $\mathbf{F^3}$ with a time constant of ~100 μs (at pH

Abbreviations: Cyt*c*O, cytochrome *c* oxidase; SUV, small unilamellar vesicle; *N*- and *P*-sides, refer to the (relatively) negatively and positively charged sides of the membrane, respectively. Time constants are given as (rate constant)$^{-1}$. Unless indicated otherwise, the amino-acid residue numbering refers to the *Rhodobacter sphaeroides* cytochrome aa_3 sequence

* Corresponding author. Fax: +46 8 153679.
E-mail address: peterb@dbb.su.se (P. Brzezinski).

0005-2728/$ - see front matter © 2007 Elsevier B.V. All rights reserved.
doi:10.1016/j.bbabio.2007.02.023

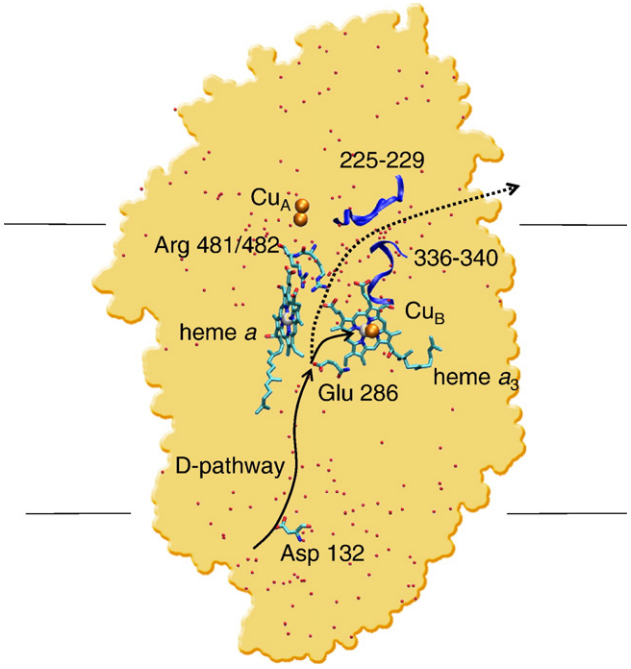

Fig. 1. The structure of cytochrome *c* oxidase from *R. sphaeroides*. The arrows indicate the proton-transfer trajectories. The D pathway starts at D132 and leads to E286. Thereafter the trajectory forks where one branch leads to the catalytic site (heme a_3 and Cu_B) and the other to the pump site, presumably around the heme a_3 D-ring propionate, Arg481 and Arg482. Above this region the pathway is not well defined and there is a large number of crystallographically resolved water molecules (red dots) and protonatable amino-acid residues. One possible exit route, lining peptides 320–340 (a part of the peptide, 336–340 is shown) in subunit I and 225–229 in subunit II, is indicated by the dotted arrow. The figure was prepared from PDB ID 1M56 using the VMD software [31].

7) concomitantly with a fractional electron transfer from Cu_A to heme *a*. In the last step the oxidized state $\mathbf{O^4}$ is formed with a time constant of ~1 ms, as another proton is taken up from the *N*-side bulk solution and an electron is transferred to the catalytic site. The $\mathbf{P^3 \rightarrow F^3}$ and the $\mathbf{F^3 \rightarrow O^4}$ transitions are each associated with pumping of one proton from the *N*- to the *P*-side of the membrane [8,9].

Both the steady-state turnover rate of the Cyt*c*O catalytic reaction and the rates of specific reaction steps associated with proton uptake and pumping display pH-dependent kinetics when studied in detergent solution (i.e. the pH is varied simultaneously on all surfaces of the protein) [10–14]. For example, with the *R. sphaeroides* cytochrome aa_3 the $\mathbf{P^3 \rightarrow F^3}$ rate decreases with increasing pH displaying a pK_a of ~9.4 [15]. The $\mathbf{F^3 \rightarrow O^4}$ transition rate titrates in a broader pH range and decreases with increasing pH displaying two pK_as of ~6.3 and 8.9 [14,16]. Because protons are taken up from the *N*-side it is likely that when Cyt*c*O sits in a membrane the pH on the *N*-side influences the reaction rates. In an earlier study Sharpe et al. [17] investigated the effect of pH gradients on the reaction catalyzed by CytcO and found that the catalytic site is in proton equilibrium with the inside of the vesicles. However, the effect on the rates of individual reaction steps of changes in pH specifically on the N- or P-side of the membrane has not been investigated previously. The issue is important because identification of the location of the proton-binding sites that interact with the redox sites is likely to facilitate identification of the structural elements involved in proton pumping. As proton pumping requires a close link between proton uptake from the *N*-side and release to the *P*-side in principle also the pH on the outside could influence the reaction. To address this question we have investigated the kinetics of internal electron-transfer reactions that are linked to proton uptake and pumping under conditions where the pH was adjusted to different values on different sides of the membrane.

Our results show that in the pH range 6–9.5 the pH on the inside of the vesicles (*N*-side) fully determines the rates of reaction steps linked to proton pumping and the kinetics is insensitive to the pH on the outside of the vesicles.

2. Materials and methods

2.1. Purification of cytochrome c oxidase

Histidine-tagged Cyt*c*O, expressed in *R. sphaeroides*, was purified using histidine-affinity chromatography as described in [18]. After purification, the buffer was exchanged to 0.1 M HEPES at pH 7.4, 0.1% dodecyl-β-D-maltoside and then the sample was rapidly frozen in liquid nitrogen. The Cyt*c*O was stored at −80 °C until use.

2.2. Reconstitution of cytochrome c oxidase into SUVs

Purified Cyt*c*O at a concentration of at least 20 μM was diluted to 4–8 μM in a buffer containing 4% (w/v) cholate and 0.15 M KCl and 25 mM phenol red. A lipid extract from Soybean L-lecitin (Sigma, type II) was made by precipitation with acetone and then extraction with diethyl ether. A lipid solution was prepared at a concentration of 40 mg/ml in a buffer containing 2% (w/v) cholate and 0.15 M KCl and 25 mM phenol red at pH 7.4. Then the lipids were sonicated under N_2 atmosphere, while kept on ice, using a tip-sonicator (Microson ultrasonic cell disruptor XL, Novakemi AB) at 50% energy output during repetitive cycles of 30 s on and 30 s off for 2 min/ml. After sonication, the SUVs were centrifuged at 1500×*g* for 20 min to remove titanium particles and lipid aggregates.

The Cyt*c*O-containing SUVs were prepared using a modified version of the protocol described in [19]. Briefly, the lipid and Cyt*c*O samples were mixed at a ratio of 1:1 and Cyt*c*O was inserted into the SUVs as detergent was removed using Bio-Beads SM-2 Adsorbent (Bio-Rad Laboratories) and a PD-10 desalting column (Amersham Pharmacia Biosciences). The pH was adjusted to a desired value, and the vesicles were stored on ice in a refrigerator overnight and used the next day after running a second PD-10 column (see also "Supplementary information").

The orientation of Cyt*c*O in the membrane was determined by comparison of the fraction reduced Cyt*c*O upon addition of a membrane-impermeable reductant (ascorbate and the redox mediator hexaammineruthenium (II) chloride (Aldrich)) and after addition of the redox mediator PMS, which results in reduction of the entire Cyt*c*O population. Approximately 75% of the Cyt*c*O population was found to be oriented with the cytochrome *c*-binding site on the outside of the SUVs.

To reduce only the "correctly oriented" Cyt*c*O population, in the experiments described in this paper the sample was reduced by ascorbate and hexaammineruthenium (II) chloride. The proton permeability of the SUVs was determined by measuring the respiratory control ratio (RCR) (see e.g. [20]). Typically, RCR values of ~10 were obtained, indicating tight SUVs.

2.3. Flow-flash measurements

The concentration of Cyt*c*O-SUVs was adjusted to 3–4 μM. The SUVs contained 150 mM KCl and 25 mM phenol red (inside the SUVs) and 150 mM KCl, 24 mM sucrose, 1 mM bis-tris propane and 100 μM EDTA (outside the SUVs). The outside pH was set to different values as indicated in the figure

legends. Then, the SUVs were transferred to an anaerobic cuvette, air was exchanged for nitrogen using a vacuum line and the Cyt*c*O was reduced by addition of 2–3 mM ascorbate and 0.5–1 μM hexaammineruthenium (II) chloride. Finally, N_2 was exchanged for CO. The sample was transferred anaerobically to one of the drive syringes of a locally modified flow-flash apparatus (Applied Photophysics, see [21] for a detailed description).

It should be noted that also CO is able to reduce Cyt*c*O [22], which means that in principle also Cyt*c*O molecules oriented with the cytochrome-*c* binding site inside the SUVs (i.e. incorrectly oriented) could become reduced. However, within the time between addition of CO and the experiment (2–4 h) oxidized Cyt*c*O becomes at most reduced to form the mixed-valence state [22] where the catalytic site is reduced while heme *a* and Cu_A are oxidized. Upon reaction with O_2 of Cyt*c*O in this state the reaction stops at state $\mathbf{P^2}$ and the transitions studied in this work do not take place. Consequently, putative reactions of the incorrectly oriented Cyt*c*O did not interfere with the investigated reactions.

The fully reduced CO-bound Cyt*c*O was mixed with an O_2-saturated buffer (~1.2 mM O_2) present in the other syringe containing 150 mM KCl, 25 mM bis-tris propane, 100 μM EDTA, at different pH at a ratio of 1:1 (see figure legends). About 300 ms after mixing the reaction was initiated by photo-dissociation of CO by a laser flash (~7 ns, 100 mJ, Nd-YAG laser, Quantel Brilliant B). Absorbance changes during the reduction of oxygen were monitored at various wavelengths (see Results and discussion).

Proton uptake from inside of the SUVs was detected using the pH-sensitive dye phenol red. In solution this dye has a pK_a of 7.5, however, when loaded into SUVs the pK_a increased by approximately 1 pH-unit (determined through titration). As the enzyme reacted with O_2, the transient absorbance changes were recorded at 556 nm, where phenol red exhibits close to maximal pH-induced absorbance changes, while the contribution of absorbance changes from Cyt*c*O is very small. In each measurement 20–30 traces were collected and averaged. As a control 3 mM FCCP was added making the membrane permeable to protons thus equilibrating the SUV inside solution with the buffer outside, thereby removing the pH dye contribution.

3. Results and discussion

Cytochrome *c* oxidase (Cyt*c*O) was incorporated into small unilamellar vesicles (SUVs) with the inside pH adjusted to different fixed values. The enzyme was reduced (four electrons per Cyt*c*O) and the sample was incubated under an atmosphere of CO. After mixing of the CO-bound Cyt*c*O-SUVs with an O_2-saturated solution having a well-defined pH (the same or different from that on the inside of the SUVs), the CO ligand was dissociated by means of a laser flash and internal electron-transfer reactions during oxidation of the reduced Cyt*c*O were studied. To investigate simultaneously proton uptake from the *N*-side of the membrane a pH dye was enclosed inside the SUVs. The rates of specific reaction steps during O_2 reduction were determined for different combinations of pH on the inside (pH_i) and outside (pH_o) of the membrane (see Table 1). In order to avoid the enzyme working against a pH gradient, which would most likely affect the results, the pH on the inside (*N*-side) was kept lower than or the same as that on the outside (*P*-side).

In cases when the pH values on the inside and outside the SUVs were different, it was essential to determine the proton leak rate to ensure that the inside pH had not changed before starting the reaction (i.e. in the time between mixing the two solutions and the laser flash). Fig. 2 shows absorbance changes at 556 nm of the pH dye phenol red encapsulated inside the vesicles after mixing the two solutions (at the time indicated by the first (leftmost) arrow). The reaction was initiated by a laser flash at $t=0$ (second arrow). The results show that the pH-change between mixing and initiation of the reaction ($t=-300$ to 0 ms) was relatively small and could be neglected, which means that the pH inside the SUVs remained close to the original value when the reaction was initiated by a laser flash.

Table 1
Dependence of $\mathbf{P^3 \rightarrow F^3}$ and $\mathbf{F^3 \rightarrow O^4}$ transition rates on the pH on the inside (pH_i, *N*-side) and outside (pH_o, *P*-side) of Cyt*c*O-SUVs

pH_i	pH_o	$P^3 \rightarrow F^3$		$F^3 \rightarrow O^4$	
		580 nm	proton uptake	445 and 580 nm	proton uptake
low	low	100 μs	300 μs	1 ms	3 ms
low	high	100 μs	300 μs	1 ms	3 ms
high	high	200 μs	not observed	2 ms/12 ms (or 3.5 ms)	6 ms

The $\mathbf{P^3 \rightarrow F^3}$ rate was determined from absorbance changes at 580 nm, while the $\mathbf{F^3 \rightarrow O^4}$ was determined from absorbance changes at 445 nm and 580 nm, at different combinations of pH_o and pH_i (low=6.0, high=9.0). Proton uptake was determined from absorbance changes of the pH dye phenol red at 556 nm, at different combinations of pH_o and pH_i (low=7.5, high=9.5). Different combinations of pH in the different experiments were used because of the limited titration range of the pH dye (~7.5–9.5). The high/low combination was not used because in this case the Cyt*c*O would work against a pH gradient, which would influence the results.

Fig. 3a shows absorbance changes at 445 nm. The first, rapid decrease ($t<100$ μs) is due to binding and cleavage of O_2 and it is not linked to proton uptake. The decrease in absorbance on a slower time scale is associated with the $\mathbf{F^3 \rightarrow O^4}$ transition. At pH_i 6.0 (red and green traces) essentially identical traces were obtained independently of pH_o ($\tau \cong 1$ ms). At pH_i 9.0 (blue trace) the $\mathbf{F^3 \rightarrow O^4}$ transition became slower and displayed a time constant of ~3.5 ms. In this case a better fit was obtained with two kinetic phases with time constants of (relative amplitudes in parentheses) 2 ms (65%) and 12 ms (35%). Such biphasic behavior has been observed previously and attributed to movement of substrate and pumped protons, respectively [23]. The biphasic behavior was found to be more pronounced with Cyt*c*O reconstituted in vesicles than in detergent-solubilized Cyt*c*O (Faxén *et al.*, unpublished data).

Fig. 3b shows absorbance changes at 580 nm upon reaction of the fully reduced Cyt*c*O with O_2. The minor decrease in absorbance seen at $t<100$ μs is due to formation of the $\mathbf{P^3}$ state ($\tau \cong 30$ μs). The reactions is not linked to proton uptake from solution or proton pumping. At pH_i 6.0 (red and green traces) it is followed by two kinetic phases with time constants of ~100 μs ($\mathbf{P^3 \rightarrow F^3}$) and ~1 ms ($\mathbf{F^3 \rightarrow O^4}$), respectively, where the latter is consistent with the observations at 445 nm discussed above. The more rapid phase is seen as a plateau or slight increase in absorbance in the time region 50–300 μs. As seen in the figure essentially identical traces were obtained, independently of pH_o (6 or 9, on the outside of the SUVs).

At pH_i 9.0 (blue trace) the increase in absorbance associated with the $\mathbf{P^3 \rightarrow F^3}$ transition was slower and it can be seen in the time range 0.1 ms to 0.4 ms ($\tau \cong 200$ μs). The next step, which is also linked to proton uptake, is seen as a decrease in the absorbance with a time constant of ~3.5 ms, i.e. slower than under conditions where pH_o was 9.0 and pH_i was 6.0. Also in this case (c.f. above) a better fit was obtained with two kinetic phases with time constants of (relative amplitudes in parentheses) 2 ms (50%) and 12 ms (50%)).

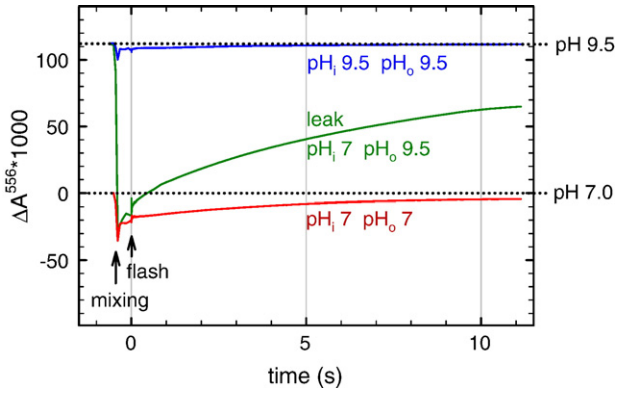

Fig. 2. Absorbance changes of phenol red enclosed within the Cyt*c*O-SUV. Three different traces are shown: inside (pH_i) and outside pH (pH_o) 9.5 (blue trace); pH_i=7 and pH_o=9.5 (green); pH_i=pH_o=7 (red). The SUVs were prepared with a fixed pH_i and a low buffer concentration on the outside. The SUV solution was mixed with another, more strongly buffered solution having the same or a different pH_o. The unresolved decrease in absorbance at time −300 ms is due to mixing of the two solutions. The zero-point on the ordinate is arbitrarily set to the absorbance at pH_i=7. The absorbance level of the blue trace is set to coincide with the absorbance level of the green trace at $t<0$ because in both cases the pH was assumed to be 9.5 inside the SUVs after "infinite time". Experimental conditions 150 mM KCl and 25 mM phenol red (pH 7.0 or 9.5) (inside the SUVs) and 150 mM KCl, 13 mM bis-tris propane (pH 7.0 or 9.5), 12 mM sucrose, 0.6 mM O_2 and 100 μM EDTA (outside the SUVs). The concentration of reacting enzyme was 0.4 μM (pH_i 7.0) or 0.6 μM (pH_i 9.5).

Fig. 3c shows absorbance changes at 556 nm of the pH-sensitive dye phenol red inside the Cyt*c*O-SUVs at pH 7.5 or 9.5. These pH values are different from those used in the measurements discussed above because they were chosen to fit within the linear part of the titration range of phenol red (the pK_a of the dye increased upon insertion into vesicles). The Cyt*c*O-SUVs with a pH_i of ~7.5 were mixed with buffers at pH_o 7.5 or pH 9.5 (red and green traces, respectively). Furthermore, Cyt*c*O-SUVs with a pH_i of 9.5 were mixed with a buffer at pH_o 9.5 (blue trace). As seen in the figure, the traces obtained with Cyt*c*O-SUVs having pH_i of 7.5 are very similar in shape and displayed time constants of ~300 μs and ~3 ms. In contrast, when pH_i was adjusted to 9.5, only one kinetic phase was observed with a time constant of ~6 ms. Because the amplitude of this phase was small at pH 9.5, it was difficult to estimate its value. Nevertheless, on the basis of the data shown in Fig. 3c we could put an upper limit on this number of ~50% of that obtained with pH_i 7.5. Assuming that a total of four protons (1 H^+ used for O_2 reduction and 1 pumped H^+ in each of the $\mathbf{P^3 \rightarrow F^3}$ and $\mathbf{F^3 \rightarrow O^4}$ transitions [9]) are taken up from the inside of the Cyt*c*O-SUVs at pH 7.5, the extent of proton uptake at pH_i 9.5 is <2 H^+ (50% of 4 H^+). The smaller extent of proton uptake indicates that there is no proton pumping at pH 9.5, which is consistent with previous results [24,25]. In conclusion, the data presented here show that the pH inside the SUVs, i.e. the *N*-side, is alone responsible for the pH-dependence of the O_2-reduction kinetics and fully determines the kinetics of both proton uptake and electron transfer in the studied pH-interval 6–9.5. These results are consistent with those obtained from earlier steady-state experiments with the mitochondrial enzyme [17].

In the light-driven proton pump bacteriorhodopsin the protonation state (determined by the pH) of a proton-release group influences the rate of proton release and order of

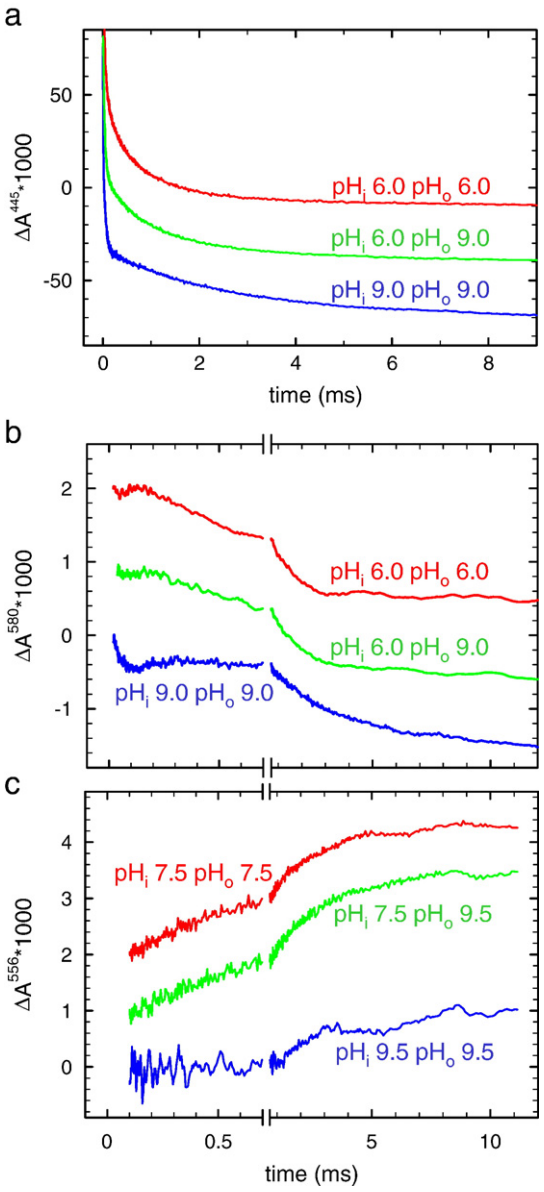

Fig. 3. (a) Absorbance changes associated with electron and proton transfer upon reaction of the fully reduced Cyt*c*O with O_2. The pH on the inside (pH_i) and outside (pH_o) was adjusted to different values as indicated in the graphs. (a) Absorbance changes at 445 nm. The decrease in absorbance at t>100 μs is associated with the $\mathbf{F^3 \rightarrow O^4}$ transition. (b) Absorbance changes at 580 nm. The initial decrease in absorbance at <100 μs is associated with formation of the $\mathbf{P^3}$ intermediate. It is followed by an increase in absorbance or a plateau associated with formation of the $\mathbf{F^3}$ intermediate. The $\mathbf{F^3 \rightarrow O^4}$ transition is seen as a decrease in absorbance at t>~300 μs. The increase in absorbance associated with $\mathbf{P^3 \rightarrow F^3}$ is seen most clearly at pH_i 9.0 (blue trace) because of the slower decay associated with the $\mathbf{F^3 \rightarrow O^4}$ transition. (c) Absorbance changes at 556 nm of the pH dye phenol red associated with proton uptake. The dye was present on the inside of the Cyt*c*O-SUVs and therefore monitored proton uptake from the *N*-side bulk solution, seen as an increase in absorbance. Experimental conditions were the same as in Fig. 2, except the differences in pH (as indicated). The concentration of reacting enzyme was ~0.8 μM (traces at pH_i 6.0 and 7.5), 1 μM (pH_i 9.0) and 0.6 μM (pH_i 9.5). In the graph all traces have been scaled to 1 μM reacting enzyme.

specific reaction steps during the photocycle [26,27], which suggests that the pH on the proton-exit side may influence the proton-release rate. In Cyt*c*O, during O_2 reduction protons are taken up through the D-pathway starting with Asp132 and leading to Glu286 (see Fig. 1). From Glu286 protons are transferred either to the catalytic site (substrate protons used for formation of water) or towards the *P*-side (protons that are pumped). In the latter case the trajectory most likely leads from Glu286 to or via the Δ-propionates of hemes *a* and a_3 (for review, see [1–4,28]). "Above" this region of the protein the trajectory transverses across an extensive network of crystallographically resolved water molecules (see Fig. 1). Despite the large number of water molecules, it appears that protons cannot exchange freely between the *P*-side and this area as evidenced from recent results using amide H/D exchange mass spectrometry, which showed that the proton access to peptides 320–340 in subunit I and 225–229 in subunit II (see Fig. 1), lining a putative proton-exit channel, varies in different states of the catalytic cycle [29]. This observation is consistent with the data from the present study, i.e. that the protonation state of the proton-release group in Cyt*c*O does not depend directly on the *P*-side pH. Furthermore, results from another recent study showed that proton release is rate limiting for electron transfer to the catalytic site during Cyt*c*O turnover [30], which would indicate that the protonation state of the proton-release group controls the rate of internal electron transfer. Assuming that the pK_a of this group is within the pH range of the measurements presented here, collectively the results would indicate that the group is not permanently in rapid equilibrium with the *P*-side bulk solution (c.f. also the results from the D/H exchange studies discussed above).

The experiments in the present study were designed such that the Cyt*c*O did not work against a proton electrochemical gradient, otherwise it would have been difficult to discriminate between effects of the gradient and changes in pH on respective sides of the membrane. In future studies we will use the same experimental approach to investigate single-turnover kinetics when Cyt*c*O works against an electrochemical gradient.

Acknowledgements

We would like to thank Pia Ädelroth and Sergei Balashov for valuable discussions. This work was supported by grants from the Swedish Research Council.

Appendix A. Supplementary data

Supplementary data associated with this article can be found, in the online version, at doi:10.1016/j.bbabio.2007.02.023.

References

[1] G. Brändén, R.B. Gennis, P. Brzezinski, Transmembrane proton translocation by cytochrome *c* oxidase, Biochim. Biophys. Acta 1757 (2006) 1052–1063.
[2] P. Brzezinski, P. Ädelroth, Design principles of proton-pumping haem-copper oxidases, Curr. Opin. Struct. Biol. 16 (2006) 465–472.
[3] M. Wikström, M.I. Verkhovsky, Towards the mechanism of proton pumping by the haem-copper oxidases, Biochim. Biophys. Acta, Bioenerg. 1757 (2006) 1047–1051.
[4] J.P. Hosler, S. Ferguson-Miller, D.A. Mills, Energy transduction: proton transfer through the respiratory complexes, Ann. Rev. Biochem. 75 (2006) 165–187.
[5] M. Svensson-Ek, J. Abramson, G. Larsson, S. Törnroth, P. Brzezinski, S. Iwata, The X-ray crystal structures of wild-type and EQ(I-286) mutant cytochrome *c* oxidases from *Rhodobacter sphaeroides*, J. Mol. Biol. 321 (2002) 329–339.
[6] L. Qin, C. Hiser, A. Mulichak, R.M. Garavito, S. Ferguson-Miller, Identification of conserved lipid/detergent-binding sites in a high-resolution structure of the membrane protein cytochrome *c* oxidase, Proc. Natl. Acad. Sci. U. S. A. 103 (2006) 16117–16122.
[7] P. Ädelroth, M. Ek, P. Brzezinski, Factors determining electron-transfer rates in cytochrome *c* oxidase: investigation of the oxygen reaction in the *R. sphaeroides* and bovine enzymes, Biochim. Biophys. Acta 1367 (1998) 107–117.
[8] M.I. Verkhovsky, J.E. Morgan, M.L. Verkhovskaya, M. Wikström, Translocation of electrical charge during a single turnover of cytochrome-c oxidase, Biochim. Biophys. Acta 1318 (1997) 6–10.
[9] K. Faxén, G. Gilderson, P. Ädelroth, P. Brzezinski, A mechanistic principle for proton pumping by cytochrome *c* oxidase, Nature 437 (2005) 286–289.
[10] P.E. Thörnström, P. Brzezinski, P.O. Fredriksson, B.G. Malmström, Cytochrome c oxidase as an electron-transport-driven proton pump: pH dependence of the reduction levels of the redox centers during turnover, Biochemistry 27 (1988) 5441–5447.
[11] D. Zaslavsky, R.C. Sadoski, K. Wang, B. Durham, R.B. Gennis, F. Millett, Single electron reduction of cytochrome *c* oxidase compound F: resolution of partial steps by transient spectroscopy, Biochemistry 37 (1998) 14910–14916.
[12] M. Oliveberg, P. Brzezinski, B.G. Malmström, The effect of pH and temperature on the reaction of fully reduced and mixed-valence cytochrome *c* oxidase with dioxygen, Biochim. Biophys. Acta 977 (1989) 322–328.
[13] I. Szundi, N. Van Eps, O. Einarsdóttir, pH dependence of the reduction of dioxygen to water by cytochrome *c* oxidase. 2. Branched electron transfer pathways linked by proton transfer, Biochemistry 42 (2003) 5074–5090.
[14] A. Namslauer, P. Brzezinski, Structural elements involved in electron-coupled proton transfer in cytochrome *c* oxidase, FEBS Lett. 567 (2004) 103–110.
[15] A. Namslauer, A. Aagaard, A. Katsonouri, P. Brzezinski, Intramolecular proton-transfer reactions in a membrane-bound proton pump: the effect of pH on the peroxy to ferryl transition in cytochrome *c* oxidase, Biochemsitry 42 (2003) 1488–1498.
[16] G. Brändén, M. Brändén, B. Schmidt, D.A. Mills, S. Ferguson-Miller, P. Brzezinski, The protonation state of a heme propionate controls electron transfer in cytochrome *c* oxidase, Biochemistry 44 (2005) 10466–10474.
[17] M.A. Sharpe, J.M. Wrigglesworth, J. Loewen, P. Nicholls, Small pH gradients inhibit cytochrome c oxidase: implications for H+ entry to the binuclear center, Biochem. Biophys. Res. Commun. 216 (1995) 931–938.
[18] D.M. Mitchell, R.B. Gennis, Rapid purification of wildtype and mutant cytochrome *c* oxidase from *Rhodobacter sphaeroides* by Ni(2+)-NTA affinity chromatography, FEBS Lett. 368 (1995) 148–150.
[19] A. Jasaitis, M.I. Verkhovsky, J.E. Morgan, M.L. Verkhovskaya, M. Wikström, Assignment and charge translocation stoichiometries of the major electrogenic phases in the reaction of cytochrome *c* oxidase with dioxygen, Biochemistry 38 (1999) 2697–2706.
[20] J. Qian, W. Shi, M. Pressler, C. Hoganson, D. Mills, G.T. Babcock, S. Ferguson-Miller, Aspartate-407 in *Rhodobacter sphaeroides* cytochrome *c* oxidase is not required for proton pumping or manganese binding, Biochemistry 36 (1997) 2539–2543.
[21] M. Brändén, H. Sigurdson, A. Namslauer, R.B. Gennis, P. Ädelroth, P. Brzezinski, On the role of the K-proton transfer pathway in cytochrome *c* oxidase, Proc. Natl. Acad. Sci. U. S. A. 98 (2001) 5013–5018.
[22] P. Brzezinski, B.G. Malmström, The reduction of cytochrome *c* oxidase by carbon monoxide, FEBS Lett. 187 (1985) 111–114.

[23] S.A. Siletsky, A.S. Pawate, K. Weiss, R.B. Gennis, A.A. Konstantinov, Transmembrane charge separation during the ferryl-oxo→oxidized transition in a nonpumping mutant of cytochrome *c* oxidase, J. Biol. Chem. 279 (2004) 52558–52565.

[24] M. Verkhovskaya, M. Verkhovsky, M. Wikström, pH dependence of proton translocation by *Escherichia coli*, J. Biol. Chem. 267 (1992) 14559–14562.

[25] G. Capitanio, P.L. Martino, N. Capitanio, E. De Nitto, S. Papa, pH dependence of proton translocation in the oxidative and reductive phases of the catalytic cycle of cytochrome *c* oxidase. The role of H2O produced at the oxygen-reduction site, Biochemistry 45 (2006) 1930–1937.

[26] L. Zimanyi, G. Varo, M. Chang, B. Ni, R. Needleman, J.K. Lanyi, Pathways of proton release in the bacteriorhodopsin photocycle, Biochemistry 31 (1992) 8535–8543.

[27] S.P. Balashov, Protonation reactions and their coupling in bacteriorhodopsin, Biochim. Biophys. Acta 1460 (2000) 75–94.

[28] D.A. Mills, S. Ferguson-Miller, Influence of structure, pH and membrane potential on proton movement in cytochrome oxidase, Biochim. Biophys. Acta 1555 (2002) 96–100.

[29] L.S. Busenlehner, L. Salomonsson, P. Brzezinski, R.N. Armstrong, Mapping protein dynamics in catalytic intermediates of the redox-driven proton pump cytochrome *c* oxidase, Proc. Natl. Acad. Sci. U. S. A. 103 (2006) 15398–15403.

[30] L. Salomonsson, K. Faxén, P. Ädelroth, P. Brzezinski, The timing of proton migration in membrane-reconstituted cytochrome *c* oxidase, Proc. Natl. Acad. Sci. U. S. A. 102 (2005) 17624–17629.

[31] W. Humphrey, A. Dalke, K. Schulten, VMD: visual molecular dynamics, J. Mol. Graph. 14 (1996) 33.